

Interaction of Acetonitrilebis(cyclopentadienyl)molybdenum(II) or Tris(acetonitrile)tricarbonylmolybdenum(0) with Tetrafluoroboric Acid in Acetonitrile. X-Ray Crystal Structures of $[\text{Mo}^{\text{IV}}(\eta^5\text{-C}_5\text{H}_5)_2(\text{MeCN})(\text{NH}=\text{CHMe})][\text{BF}_4]_2$, $[\text{Mo}^{\text{IV}}(\eta^5\text{-C}_5\text{H}_5)_2(\text{PMe}_3)_2][\text{BF}_4]_2$, $[\text{Mo}^0(\text{CO})_2(\text{MeCN})_3(\eta^3\text{-CH}_2\text{CHNH}_2)]\text{BF}_4$, and $[\text{Mo}^{\text{III}}_2(\mu\text{-O})(\text{MeCN})_{10}][\text{BF}_4]_4$ †

Brian S. McGilligan, Thomas C. Wright, and Geoffrey Wilkinson*
Chemistry Department, Imperial College of Science and Technology, London SW7 2AY
Majid Motevalli and Michael B. Hursthouse*
Chemistry Department, Queen Mary College, London EC1 4NS

The interaction of $\text{Mo}(\eta^5\text{-C}_5\text{H}_5)_2(\text{MeCN})$ with $\text{HBF}_4\cdot\text{Et}_2\text{O}$ in MeCN gives the molybdenum(IV) complex $[\text{Mo}(\eta^5\text{-C}_5\text{H}_5)_2(\text{MeCN})(\text{NH}=\text{CHMe})][\text{BF}_4]_2$ (2) which on substitution with PMe_3 gives $[\text{Mo}(\eta^5\text{-C}_5\text{H}_5)_2(\text{PMe}_3)_2][\text{BF}_4]_2$ (3). Similar protonation of $\text{Mo}(\text{CO})_3(\text{MeCN})_3$ under hydrogen gives the complex $[\text{Mo}(\text{CO})_2(\text{MeCN})_3(\eta^3\text{-CH}_2\text{CHNH}_2)]\text{BF}_4$ (4) and in the presence of oxygen the molybdenum(III) complex $[\text{Mo}_2(\mu\text{-O})(\text{MeCN})_{10}][\text{BF}_4]_4$ (5). X-Ray crystal structures of compounds (2), (3), (4), and (5) are reported.

The η^2 -bonding of acetonitrile, long proposed on the basis of infrared spectra has been confirmed by an X-ray study of $\text{Mo}(\eta^5\text{-C}_5\text{H}_5)_2(\text{MeCN})$.¹ In view of reactions of methanol with $[\text{Cr}(\text{MeCN})_2(\text{dmpe})_2]^{2+}$ [dmpe = 1,2-bis(dimethylphosphino)ethane], which lead to compounds with $\sigma\text{-NEt}$ and $\sigma\text{-N}=\text{CHMe}$ groups,² we have studied the protonation of $\text{Mo}(\eta^5\text{-C}_5\text{H}_5)_2(\text{MeCN})$ and of $\text{Mo}(\text{CO})_3(\text{MeCN})_3$ by tetrafluoroboric acid.

Results and Discussion

1. *Protonation of $\text{Mo}(\eta^5\text{-C}_5\text{H}_5)_2(\text{MeCN})$.*—The interaction of a related CF_3CN complex with hydrogen chloride³ gives rise to an iminium salt (1), the structure of which was proposed on the basis of spectroscopic data. However, the interaction of the acetonitrile complex with $\text{HBF}_4\cdot\text{Et}_2\text{O}$ gives the molybdenum(IV) imino complex (2) as the tetrafluoroborate, $[\text{Mo}(\eta^5\text{-C}_5\text{H}_5)_2(\text{MeCN})(\text{NH}=\text{CHMe})][\text{BF}_4]_2$ whose structure has been determined by X-ray diffraction.

A diagram of the molecular structure is shown in Figure 1: important bond lengths and angles are given in Table 1. The molecule lies on a crystallographic mirror plane, which contains both the acetonitrile and the imino ligand, and requires an exactly eclipsed orientation of the $\text{Mo}(\eta^5\text{-C}_5\text{H}_5)_2$ system. The acetonitrile ligand has normal geometry with almost linear bonding to the metal. The imino ligand is bent at both the nitrogen and α -carbon, where protonation has occurred, but the angles (see Table 1) are much larger than would be expected for the formal sp^2 hybridisation at these centres. Furthermore, the formally $\text{C}=\text{N}$ double bond is very short, being very similar in length to the triple bond in the acetonitrile ligand. The coordination of this ligand to Mo appears to be marginally weaker than that of the acetonitrile, as judged from the Mo–N distances.

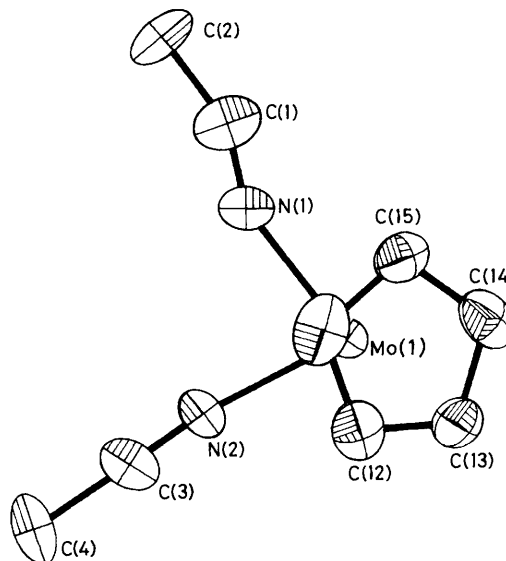


Figure 1. Structure of the cation in $[\text{Mo}(\eta^5\text{-C}_5\text{H}_5)_2(\text{MeCN})(\text{NH}=\text{CHMe})][\text{BF}_4]_2$ (2)

The imino complex ion is relatively inert to substitution and there is no exchange with CD_3CN . However, interaction with PMe_3 gives the complex $[\text{Mo}(\eta^5\text{-C}_5\text{H}_5)_2(\text{PMe}_3)_2][\text{BF}_4]_2$ (3) whose structure has also been determined. While two other complexes of this type, with PMe_2Ph^4 and $\text{Ph}_2\text{PCH}_2\text{CH}_2\text{-PPh}_2$,⁵ are known, these have not been structurally characterised. A diagram of this cation, which is also sited on a crystallographic mirror plane, is shown in Figure 2: bond lengths and angles are given in Table 2. The orientation of the cation is such that the mirror plane bisects the P–Mo–P angle and each of the two cyclopentadienyl rings. The P–Mo–P angle is somewhat larger than the N–Mo–N angle in compound (2), as is consistent with the greater size of the phosphine ligands. The $\eta^5\text{-C}_5\text{H}_5$ ligands also show some tilt (*cf.* spread of $\text{Mo}\cdots\text{C}$ distances), again as a result of steric effects.

The mechanism of the reduction of the $\eta^2\text{-MeCN}$ ligand in $\text{Mo}(\eta^5\text{-C}_5\text{H}_5)_2(\text{MeCN})$ by protons is presumably similar to

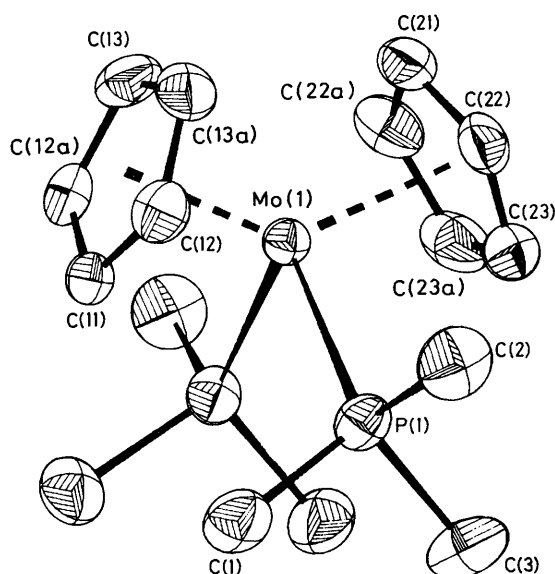
† Acetonitrilebis(η^5 -cyclopentadienyl)(ethanimine)molybdenum(IV) bis(tetrafluoroborate), bis(η^5 -cyclopentadienyl)bis(trimethylphosphine)molybdenum(IV) bis(tetrafluoroborate), tris(acetonitrile)-bis(carbonyl)(η^3 -vinylammonium)molybdenum(0) tetrafluoroborate, and decakis(acetonitrile)(μ -oxo)-dimolybdenum(III) tetrakis(tetrafluoroborate).

Supplementary data available: see Instructions for Authors, *J. Chem. Soc., Dalton Trans.*, 1988, Issue 1, pp. xvii–xx.

Table 1. Selected bond lengths (Å) and angles (°) for $[\text{Mo}(\eta^5\text{-C}_5\text{H}_5)_2(\text{MeCN})(\text{NH}=\text{CHMe})][\text{BF}_4]_2$ (2)

N(1)–Mo(1)	2.145(11)	N(2)–Mo(1)	2.125(11)
C(11)–Mo(1)	2.229(11)	C(12)–Mo(1)	2.302(11)
C(13)–Mo(1)	2.347(11)	C(14)–Mo(1)	2.331(11)
C(15)–Mo(1)	2.275(11)	C(1)–N(1)	1.097(15)
C(3)–N(2)	1.095(16)	C(2)–C(1)	1.445(18)
C(4)–C(3)	1.456(19)	C(12)–C(11)	1.376(15)
C(15)–C(11)	1.384(15)	C(13)–C(12)	1.336(14)
C(14)–C(13)	1.393(13)	C(15)–C(14)	1.386(14)
N(2)–Mo(1)–N(1)	80.4(5)	C(1)–N(1)–Mo(1)	153.9(12)
Cp(1)–Mo(1)–Cp(1a)*	133.7(5)	C(3)–N(2)–Mo(1)	173.1(12)
C(2)–C(1)–N(1)	155.3(19)	C(15)–C(11)–C(12)	106.3(10)
C(4)–C(3)–N(2)	177.3(17)	C(14)–C(13)–C(12)	109.1(10)
C(13)–C(12)–C(11)	109.7(10)	C(14)–C(15)–C(11)	109.0(10)
C(15)–C(14)–C(13)	105.8(10)		

* Cp(1) is defined as the midpoint of C(11), C(12), C(13), C(14), C(15). Key to symmetry operations relating designated atoms to reference atoms at (x, y, z): (a) z, 0.5 – y, z.

**Figure 2.** Structure of the cation in $[\text{Mo}(\eta^5\text{-C}_5\text{H}_5)_2(\text{PMe}_3)_2][\text{BF}_4] \cdot \text{MeCN}$ (3)

other hydride transfers² and probably involves initial protonation at the metal followed by hydrogen shifts (see Scheme, $\eta^5\text{-C}_5\text{H}_5$ ligands omitted).

2. Protonation of $\text{Mo}(\text{CO})_3(\text{MeCN})_3$.—The interaction of this carbonyl complex in MeCN with $\text{HBF}_4 \cdot \text{OEt}_2$ occurs with effervescence and loss of CO and H_2 to give the orange complex $[\text{Mo}(\text{CO})_2(\text{MeCN})_3(\eta^3\text{-CH}_2\text{CHNH}_2)]\text{BF}_4$ (4) and green $[\text{Mo}_2(\mu\text{-O})(\text{MeCN})_{10}][\text{BF}_4]_4$ (5).

Under nitrogen or argon atmospheres the yields of (4) and (5) are ca. 46 and 25% respectively; despite attempts to exclude water and oxygen in the reaction the oxo species was always observed. However, the yields of (4) can be substantially increased (to 76%) when the reaction is carried out under dihydrogen, while under air (5) can be obtained in high yield (88%).

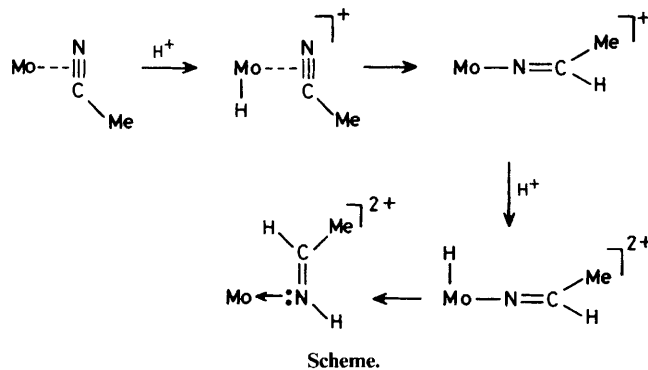
The aza-allylic species is diamagnetic and is a 1:1 electrolyte in acetonitrile. The structure of the cation determined by X-ray

Table 2. Bond lengths (Å) and angles (°) for $[\text{Mo}(\eta^5\text{-C}_5\text{H}_5)_2(\text{PMe}_3)_2][\text{BF}_4]_2 \cdot \text{MeCN}$ (3)*

P(1)–Mo(1)	2.515(5)	C(11)–Mo(1)	2.268(11)
C(12)–Mo(1)	2.298(9)	C(13)–Mo(1)	2.330(9)
C(21)–Mo(1)	2.275(13)	C(22)–Mo(1)	2.305(9)
C(23)–Mo(1)	2.327(10)	C(1)–P(1)	1.805(10)
C(2)–P(1)	1.816(11)	C(3)–P(1)	1.806(12)
C(12)–C(11)	1.406(11)	C(13)–C(13a)	1.386(18)
C(22)–C(21)	1.414(11)	C(12)–C(13a)	1.378(11)
C(23)–C(23a)	1.347(20)	C(23)–C(22)	1.385(12)
F(2)–B(1)	1.354(10)	F(1)–B(1)	1.348(10)
F(4)–B(1)	1.341(10)	F(3)–B(1)	1.335(11)
C(01)–C(01)	1.434(16)	C(01)–N(01)	1.118(14)
Cp(1)–Mo(1)–Cp(2)	134.2(2)	Cp(1)–Mo(1)–P(1)	106.7(4)
Cp(2)–Mo(1)–P(1)	104.8(4)	C(1)–P(1)–Mo(1)	116.2(4)
C(2)–P(1)–Mo(1)	112.1(4)	C(2)–P(1)–C(1)	102.9(5)
C(3)–P(1)–Mo(1)	120.6(4)	C(3)–P(1)–C(1)	99.7(6)
C(3)–P(1)–C(2)	102.9(6)	P(1)–Mo(1)–P(1a)	91.6(2)
F(2)–B(1)–F(1)	110.3(9)	F(3)–B(1)–F(1)	108.8(8)
F(3)–B(1)–F(2)	110.8(8)	F(4)–B(1)–F(1)	107.4(8)
F(4)–B(1)–F(2)	108.1(8)	F(4)–B(1)–F(3)	11.4(9)
C(02)–C(01)–N(01)	177.5(16)		

* Cp(1) is defined as the midpoint of C(11), C(12), C(13), C(12a), C(13a). Cp(2) is defined as the midpoint of C(21), C(22), C(23), C(22a), C(23a).

Key to symmetry operations relating designated atoms to reference atoms at (x, y, z): (a) x, 0.5 – y, z.



Scheme.

study is shown in Figure 3 while bond lengths and angles are given in Table 3. The $\eta^3\text{-CH}_2\text{CHNH}_2^+$ ligand, when regarded as occupying one co-ordination site, leads to the geometry about molybdenum(0) being most conveniently described as octahedral.

Although the refinement of the structure seems to indicate a localised C–C–N arrangement for the aza-allyl, the near equivalence of the C–C and C–N bonds and the Mo–N, Mo–C bonds, suggests that C–C–N, N–C–C disorder may be present. However, although the outer Mo–C, Mo–N distances are slightly longer than the inner Mo–C distance, the true η^3 -mode of allyl bonding is emphasised by the angles between the aza-allyl plane C(6), C(5), N(4), and the 'equatorial plane' formed by Mo, C(2), C(1), N(1), N(3) [$14.2(1)^\circ$], or the No–N(2) line [$83.5(1)^\circ$].

A similar type of ligand, $\eta^3\text{-CH}_2\text{C}(\text{Ph})\text{NHMe}^+(\text{L})$, in $[\text{Mo}(\eta^5\text{-C}_5\text{H}_5)(\text{CO})_2\text{L}]^+$ has been made by methylation of an aza-allyl by $\text{CF}_3\text{SO}_3\text{Me}$.⁶

The way in which the aza-allyl cation is formed is clearly very complicated; it seems likely that the molecular hydrogen generated by acid oxidation of $\text{Mo}(\text{CO})_3(\text{MeCN})_3$ is involved

Table 3. Selected bond lengths (Å) and angles (°) for $[\text{Mo}(\text{CO})_2(\text{MeCN})_3(\eta^2\text{-CH}_2\text{CHNH}_2)]\text{BF}_4$ (4)

N(1)–Mo(1)	2.226(11)	C(21)–N(2)	1.107(13)	N(2)–Mo(1)	2.170(11)	C(211)–C(21)	1.496(19)
N(3)–Mo(1)	2.227(7)	C(31)–N(3)	1.123(8)	C(1)–Mo(1)	1.931(8)	C(311)–C(31)	1.459(10)
C(2)–Mo(1)	1.956(11)	O(11)–C(1)	1.178(9)	N(4)–Mo(1)	2.321(9)	O(21)–C(2)	1.148(11)
C(5)–Mo(1)	2.198(9)	C(5)–N(4)	1.401(12)	C(6)–Mo(1)	2.313(11)	C(6)–C(5)	1.392(14)
C(11)–N(1)	1.141(13)			C(111)–C(11)	1.438(17)		
N(2)–Mo(1)–N(1)	81.5(3)	C(6)–Mo(1)–N(2)	152.1(4)	N(3)–Mo(1)–N(1)	79.3(4)	C(6)–Mo(1)–N(3)	118.6(5)
N(3)–Mo(1)–N(2)	76.9(4)	C(6)–Mo(1)–C(1)	70.1(5)	C(1)–Mo(1)–N(1)	99.8(5)	C(6)–Mo(1)–C(2)	110.0(4)
C(1)–Mo(1)–N(2)	93.7(5)	C(6)–Mo(1)–N(4)	61.3(4)	C(1)–Mo(1)–N(3)	170.6(3)	C(6)–Mo(1)–C(5)	35.8(3)
C(2)–Mo(1)–N(1)	169.3(4)	C(11)–N(1)–Mo(1)	171.7(11)	C(2)–Mo(1)–N(2)	87.9(4)	C(111)–C(11)–N(1)	177.1(13)
C(2)–Mo(1)–N(3)	100.1(4)	C(21)–N(2)–Mo(1)	172.9(11)	C(2)–Mo(1)–C(1)	79.0(5)	C(211)–C(21)–N(2)	177.2(14)
N(4)–Mo(1)–N(1)	120.3(4)	C(31)–N(3)–Mo(1)	167.2(5)	N(4)–Mo(1)–N(2)	146.6(4)	C(311)–C(31)–N(3)	178.3(15)
N(4)–Mo(1)–N(3)	82.5(3)	O(11)–C(1)–Mo(1)	178.0(8)	N(4)–Mo(1)–C(1)	105.7(4)	O(21)–C(2)–Mo(1)	176.8(7)
N(4)–Mo(1)–C(2)	70.0(4)	C(5)–N(4)–Mo(1)	67.2(5)	C(5)–Mo(1)–N(1)	86.1(4)	N(4)–C(5)–Mo(1)	76.8(5)
C(5)–Mo(1)–N(2)	160.4(3)	C(6)–C(5)–Mo(1)	76.6(6)	C(5)–Mo(1)–N(3)	86.0(4)	C(6)–C(5)–N(4)	115.6(8)
C(5)–Mo(1)–C(1)	103.3(4)	C(5)–C(6)–Mo(1)	67.5(5)	C(5)–Mo(1)–C(2)	104.6(4)		
C(5)–Mo(1)–N(4)	36.0(3)			C(6)–Mo(1)–N(1)	79.2(4)		

Table 4. Bond lengths (Å) and angles (°) for $[\text{Mo}_2(\mu\text{-O})(\text{MeCN})_{10}][\text{BF}_4]_4 \cdot 2\text{MeCN}$ (5)

O(1)–Mo(1)	1.847(3)	C(8)–C(7)	1.427(12)	N(1)–Mo(1)	2.121(9)	C(10)–C(9)	1.438(14)
N(2)–Mo(1)	2.114(8)	F(1)–B(1)	1.255(14)	N(3)–Mo(1)	2.134(8)	F(2)–B(1)	1.251(16)
N(4)–Mo(1)	2.112(8)	F(3)–B(1)	1.304(16)	N(5)–Mo(1)	2.164(9)	F(4)–B(1)	1.260(17)
C(1)–N(1)	1.113(11)	F(5)–B(2)	1.250(14)	C(3)–N(2)	1.131(10)	F(6)–B(2)	1.275(17)
C(5)–N(3)	1.124(10)	F(7)–B(2)	1.213(14)	C(7)–N(4)	1.142(10)	F(8)–B(2)	1.185(16)
C(9)–N(5)	1.141(11)	C(01)–N(01)	1.097(19)	C(2)–C(1)	1.460(14)	C(02)–C(01)	1.354(19)
C(4)–C(3)	1.419(13)			C(6)–C(5)	1.437(12)		
N(1)–Mo(1)–O(1)	91.3(3)	N(5)–Mo(1)–N(4)	90.3(3)	N(2)–Mo(1)–O(1)	92.9(3)	C(1)–N(1)–Mo(1)	179.2(7)
N(2)–Mo(1)–N(1)	175.7(2)	C(3)–N(2)–Mo(1)	177.2(7)	N(3)–Mo(1)–O(1)	94.0(3)	C(5)–N(3)–Mo(1)	176.4(7)
N(3)–Mo(1)–N(1)	90.1(3)	C(7)–N(4)–Mo(1)	175.0(6)	N(3)–Mo(1)–N(2)	88.9(3)	C(9)–N(5)–Mo(1)	173.5(7)
N(4)–Mo(1)–O(1)	90.0(3)	C(2)–C(1)–N(1)	178.6(10)	N(4)–Mo(1)–N(1)	89.0(3)	C(4)–C(3)–N(2)	178.9(9)
N(4)–Mo(1)–N(2)	91.7(3)	C(6)–C(5)–N(3)	178.4(9)	N(4)–Mo(1)–N(3)	175.9(3)	C(8)–C(7)–N(4)	178.3(9)
N(5)–Mo(1)–O(1)	179.2(2)	C(10)–C(9)–N(5)	178.2(10)	N(5)–Mo(1)–N(1)	87.9(4)		
N(5)–Mo(1)–N(2)	87.8(4)			N(5)–Mo(1)–N(3)	85.7(3)		
F(2)–B(1)–F(1)	114.7(14)	F(6)–B(2)–F(5)	99.6(14)	F(3)–B(1)–F(1)	113.3(13)	F(7)–B(2)–F(5)	113.5(14)
F(3)–B(1)–F(2)	112.8(14)	F(7)–B(2)–F(6)	106.1(14)	F(4)–B(1)–F(1)	106.6(14)	F(8)–B(2)–F(5)	103.9(14)
F(4)–B(1)–F(2)	114.4(14)	F(8)–B(2)–F(6)	107.3(15)	F(4)–B(1)–F(3)	93.0(14)	F(8)–B(2)–F(7)	123.9(15)
C(02)–C(01)–N(01)	174.9(21)						

Table 5. Analytical data for molybdenum compounds

Compound	Colour	M.p./°C	Analysis (%) [*]		
			C	H	N
(2) $[\text{Mo}(\eta^5\text{-C}_5\text{H}_5)_2(\text{MeCN})(\text{NH}=\text{CHMe})][\text{BF}_4]_2$	Deep red		33.8 (34.7)	3.7 (3.7)	5.3 (5.8)
(3) $[\text{Mo}(\eta^5\text{-C}_5\text{H}_5)_2(\text{PMc}_3)_2][\text{BF}_4]_2$	Yellow	> 230 (decomp.)	34.1 (34.7)	4.9 (5.1)	
(4) $[\text{Mo}(\text{CO})_2(\text{MeCN})_3(\eta^3\text{-CH}_2\text{CHNH}_2)]\text{BF}_4$	Orange	178	29.6 (29.6)	3.5 (3.5)	13.2 (13.8)
(5) $[\text{Mo}_2(\mu\text{-O})(\text{MeCN})_{10}][\text{BF}_4]_4$	Dark green	> 140 (decomp.)	24.0 (24.8)	2.9 (3.1)	14.1 (14.5)

* Calculated values in parentheses (non-solvated compounds).

and indeed, as noted above, the yield of the aza-allyl complex is increased by carrying out the protonation in a hydrogen atmosphere. Conversion of MeCN to CH_2CHNH_2 at some point presumably involves an oxidative addition of acetonitrile as $\text{H-Mo-CH}_2\text{CN}$ for which there is ample precedent.⁷ Hydride transfers to both C and N, as in other work,² will be required.

3. *The μ -Oxo Species $[\text{Mo}_2(\mu\text{-O})(\text{MeCN})_{10}][\text{BF}_4]_4$ (5).*— This molybdenum(III) species is diamagnetic and the fluoro-borate salt is a 1:4 electrolyte in MeCN, the conductivity being similar to that for $[\text{Cr}_2(\mu\text{-O})(\text{MeCN})_2(\text{dmpe})_4][\text{BPh}_4]_4$.² The acetonitrile can be displaced by other neutral or anionic ligands and these studies will be described separately. Electrochemical studies do not indicate reversible reduction or oxidation

Table 6. Crystallographic data

(a) Crystal data

Compound	(2)	(3)	(4)	(5)
Formula	$C_{14}H_{18}B_2F_8MoN_2$	$C_{16}H_{28}B_2F_8Mo \cdot CH_3CN$	$C_{10}H_{14}BF_4MoN_4O_2$	$C_{20}H_{30}B_2F_8Mo_2N_{10} \cdot 2CH_3CN$
<i>M</i>	483.86	592.944	405.002	1 047.72
<i>a</i> /Å	13.706(3)	12.598(4)	21.809(5)	10.229(2)
<i>b</i> /Å	7.857(3)	15.357(2)	7.525(2)	22.345(5)
<i>c</i> /Å	17.278(2)	13.116(2)	10.237(2)	10.945(5)
α /°	90	90	90	90
β /°	90	90	90	110.26(3)
γ /°	90	90	90	90
<i>U</i> /Å ³	1 860.63	2 537.52	1 780.02	2 346.46
System	Orthorhombic	Orthorhombic	Orthorhombic	Monoclinic
Space group	<i>Pnma</i>	<i>Pnma</i>	<i>Pna2</i> ₁	<i>P2</i> ₁ / <i>n</i>
<i>D</i> _c /g cm ⁻³	1.73	1.55	1.601	1.48
<i>Z</i>	4	4	4	2
<i>F</i> (000)	952	1 200	792	1 040
μ (Mo- <i>K</i> _α)/cm ⁻¹	7.62	6.92	7.36	6.16

(b) Data collection

θ min., max./°	1.5, 25	1.5, 25	1.5, 25	1.5, 25
Total data measured	1 966	2 650	1 739	4 704
Total data unique	1 773	2 318	1 560	4 124
Total data observed	1 263	1 210	1 423	2 538
Significance test	$F_o > 4\sigma(F_o)$	$F_o > 4\sigma(F_o)$	$F_o > 3\sigma(F_o)$	$F_o > 5\sigma(F_o)$

(c) Refinement

No. of parameters	197	219	211	340
Weight scheme parameters, <i>g</i> ^a	0.000 03	0.000 54	0.0002	0.000 64
Final <i>R</i> ^b	0.054	0.0434	0.0267	0.0583
Final <i>R</i> ' ^c	0.066	0.0491	0.0391	0.0728

^a $w = 1/[\sigma^2(F_o) + gF_o^2]$. ^b $R = \Sigma \Delta F / \Sigma F_o$. ^c $R' = [\Sigma w(\Delta F)^2 / \Sigma wF_o^2]$.

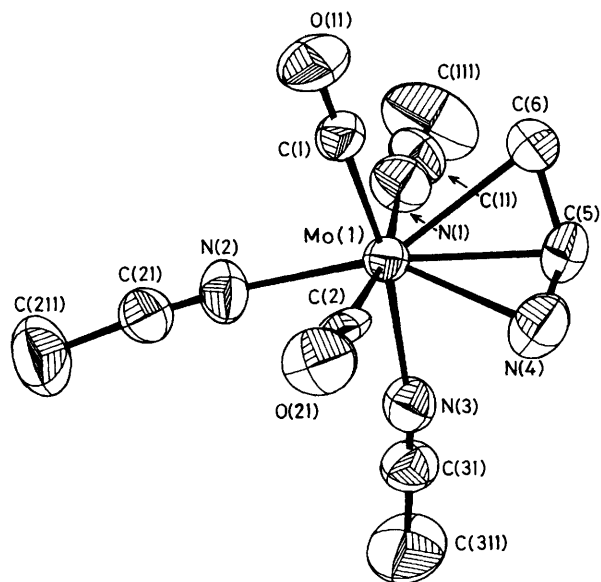


Figure 3. Structure of the cation in $[Mo(CO)_2(MeCN)_3-(\eta^3-CH_2CHNH_2)]BF_4$ (4)

phenomena. The structure of this molybdenum(III) cation is shown in Figure 4; bond lengths and angles are given in Table 4.

Although many μ -oxo compounds of molybdenum are known,⁸ these contain additional terminal Mo=O or Mo=S groups. An exception⁹ is $[Mo_2(\mu-O)(S_2CNEt_2)_6]^+$, but this ion has mixed oxidation states (mean of 4.5) and is seven-coordinate: it has an almost linear Mo–O–Mo angle (175.7°) with Mo–O = 1.849 Å. In the present μ -oxo complex the angle is

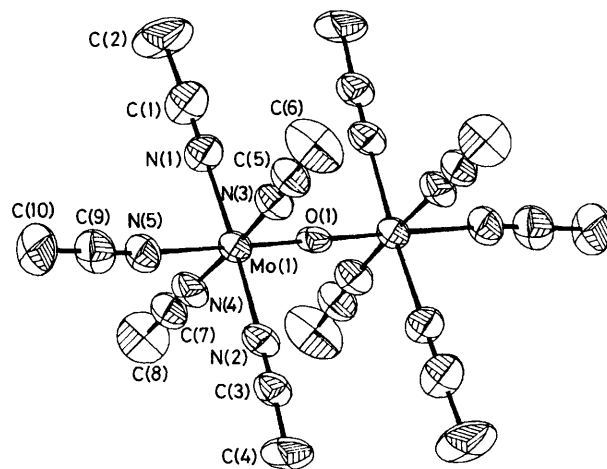


Figure 4. Structure of the cation in $[Mo_2(\mu-O)(MeCN)_{10}][BF_4]_4 \cdot 2MeCN$ (5)

exactly 180° by virtue of the centrosymmetry of the cation, indicating $d_{\pi}-p_{\pi}$ overlap as in other well known¹⁰ linear M–O–M species such as $[Ru_2(\mu-O)Cl_{10}]^{4-}$. Also consistent with this bonding mode is the unique Mo–O length of 1.847(3) Å and the eclipsed arrangement of the orthogonal MoN₄ 'equatorial plane'. The Mo–N bond *trans* to the μ -O group is only slightly longer than the distances in the equatorial plane.

Spectroscopic data are in accord with the structure as determined. The resonance-Raman spectrum closely resembles that of $[Ru_2(\mu-O)Cl_{10}]^{4-11}$ in that the M–O–M frequency is at 341.0 cm⁻¹. No ⁹⁵Mo n.m.r. signal could be detected probably because of broadening by the nitrogen quadrupole of the MeCN ligands.

Table 7. Fractional atomic co-ordinates ($\times 10^4$) for $[\text{Mo}(\eta^5\text{-C}_5\text{H}_5)_2(\text{MeCN})(\text{NH}=\text{CHMe})][\text{BF}_4]_2$ (2)

Atom	x	y	z
Mo(1)	2 213(1)	2 500*	1 232(1)
N(1)	2 068(7)	2 500*	-4(6)
N(2)	3 711(7)	2 500*	914(6)
C(1)	1 650(13)	2 500*	-546(8)
C(2)	1 527(13)	2 500*	-1 377(8)
C(3)	4 503(10)	2 500*	825(8)
C(4)	5 546(11)	2 500*	668(11)
C(11)	2 344(10)	-304(12)	1 065(6)
C(12)	2 717(7)	-10(13)	1 792(6)
C(13)	2 012(8)	569(14)	2 256(5)
C(14)	1 139(7)	635(14)	1 844(6)
C(15)	1 355(8)	36(13)	1 109(6)
B(1)	8 622(12)	2 500*	1 008(8)
F(11)	8 903(7)	2 500*	1 731(5)
F(12)	9 115(7)	1 323(12)	621(5)
F(13)	7 760(7)	2 500*	884(7)
B(2)	-367(17)	2 500*	6 470(13)
F(21)	631(19)	2 500*	6 057(16)
F(22)	-1 093(14)	2 500*	6 098(12)
F(23)	204(16)	1 275(25)	6 235(12)
F(24)	-220(15)	771(24)	6 676(11)
F(25)	-19(21)	2 500*	7 235(16)
F(26)	-1 004(22)	2 500*	7 017(18)

* Invariant parameter. Occupancies of fluorines on B(2): F(21) 0.72, F(22) 0.69, F(23) 0.69, F(24) 0.67, F(25) 0.62, F(26) 0.61.

Table 8. Fractional atomic co-ordinates ($\times 10^4$) for $[\text{Mo}(\eta^5\text{-C}_5\text{H}_5)_2(\text{PMe}_3)_2][\text{BF}_4]_2 \cdot \text{MeCN}$ (3)

Atom	x	y	z
Mo(1)	1 980(1)	2 500*	225(1)
P(1)	3 165(2)	3 674(1)	928(2)
C(11)	1 242(9)	2 500*	1 802(7)
C(12)	841(6)	3 235(6)	1 290(6)
C(13)	235(6)	2 049(6)	481(6)
C(21)	1 335(10)	2 500*	-1 395(8)
C(22)	1 978(8)	1 750(6)	-1 297(5)
C(23)	3 000(7)	2 062(6)	-1 162(6)
C(1)	3 156(8)	3 808(6)	2 295(6)
C(2)	2 791(8)	4 747(5)	470(7)
C(3)	4 579(8)	3 647(7)	705(8)
B(1)	-443(8)	670(6)	-2 278(6)
F(1)	216(5)	977(4)	-3 003(4)
F(2)	110(5)	220(3)	-1 567(4)
F(3)	-1 174(5)	165(4)	-2 718(4)
F(4)	-889(5)	1 360(4)	-1 820(4)
N(01)	2 252(12)	2 500*	4 239(8)
C(01)	2 146(10)	2 500*	5 085(9)
C(02)	2 059(11)	2 500*	6 176(8)

* Invariant parameter.

Experimental

The general techniques and spectroscopic methods were as previously described.² Raman spectra were determined on a Spex Ramalog 5 with Datamate acquisition unit.

Analytical data (Pascher Laboratories) are collected in Table 5. N.m.r. data are in p.p.m. referenced to SiMe_4 with coupling constants in Hz.

1. *Interaction of $\text{Mo}(\eta^5\text{-C}_5\text{H}_5)_2(\eta^2\text{-MeCN})$ with Tetrafluoroboric acid.*—To $\text{Mo}(\eta^5\text{-C}_5\text{H}_5)_2(\text{MeCN})^1$ (0.5 g, 1.9 mmol) in MeCN (50 cm^3) was added $\text{HBF}_4 \cdot \text{Et}_2\text{O}$ (2 cm^3 , 50%). Although the reaction is rapid the solution was stirred for ca. 1 h, reduced to 7–10 cm^3 , and extracted several times with Et_2O to remove

Table 9. Fractional atomic co-ordinates ($\times 10^4$) for $[\text{Mo}(\text{CO})_2(\text{MeCN})_3(\eta^3\text{-CH}_2\text{CHNH}_2)]\text{BF}_4$ (4)

Atom	x	y	z
Mo(1)	2 712(0.5)	6 888(1)	5 000*
N(1)	3 431(4)	7 399(14)	6 497(8)
C(11)	3 800(4)	7 445(14)	7 288(8)
C(111)	4 283(5)	7 552(21)	8 240(13)
N(2)	3 471(5)	7 465(14)	3 695(7)
C(21)	3 881(5)	7 597(15)	3 068(9)
C(211)	4 429(5)	7 691(17)	2 190(13)
N(3)	3 225(2)	4 331(6)	4 941(10)
C(31)	3 574(2)	3 236(7)	4 950(15)
C(311)	4 038(4)	1 838(9)	4 930(23)
C(1)	2 367(3)	9 243(8)	4 851(10)
O(11)	2 142(2)	10 659(6)	4 739(7)
C(2)	2 194(3)	6 610(6)	3 454(8)
O(21)	1 881(3)	6 527(7)	2 555(6)
N(4)	1 893(3)	5 026(9)	5 470(8)
C(5)	2 180(3)	5 687(11)	6 594(7)
C(6)	2 113(4)	7 503(13)	6 809(8)
B	5 306(4)	7 134(14)	5 344(11)
F(1)	4 882(3)	5 842(6)	5 261(9)
F(2)	5 580(4)	7 136(15)	6 514(10)
F(3)	5 721(4)	6 993(18)	4 424(13)
F(4)	5 016(5)	8 687(8)	5 267(13)

* Invariant parameter.

Table 10. Fractional atomic co-ordinates ($\times 10^4$) for $[\text{Mo}_2(\mu\text{-O})(\text{MeCN})_{10}][\text{BF}_4]_4 \cdot 2\text{MeCN}$ (5)

Atom	x	y	z
Mo(1)	4 162(1)	5 570(0.5)	704(1)
O(1)	5 000*	5 000*	0*
N(1)	5 594(7)	6 233(3)	574(6)
N(2)	2 683(6)	4 956(3)	917(6)
N(3)	5 454(7)	5 384(3)	2 664(6)
N(4)	2 834(6)	5 809(3)	-1 185(6)
N(5)	3 208(7)	6 246(3)	1 538(6)
C(1)	6 347(10)	6 582(4)	520(8)
C(2)	7 321(12)	7 040(6)	414(12)
C(3)	1 881(8)	4 643(4)	1 064(7)
C(4)	857(10)	5 254(5)	1 224(10)
C(5)	6 122(9)	5 315(4)	3 712(8)
C(6)	6 941(10)	5 231(6)	5 062(9)
C(7)	2 188(8)	5 922(4)	-2 240(8)
C(8)	1 411(11)	6 053(5)	-3 571(9)
C(9)	2 797(9)	6 588(4)	2 090(8)
C(10)	2 322(11)	7 023(5)	2 811(10)
B(1)	5 177(12)	6 543(7)	-3 490(12)
B(2)	10 339(12)	4 258(7)	7 199(11)
F(1)	6 472(8)	6 505(5)	-2 930(11)
F(2)	4 583(10)	6 056(5)	-3 903(13)
F(3)	4 561(12)	6 848(6)	-2 831(12)
F(4)	4 973(13)	6 943(7)	-4 347(11)
F(5)	9 037(10)	4 261(6)	6 729(11)
F(6)	10 586(14)	3 794(6)	6 638(11)
F(7)	10 791(13)	4 152(7)	8 358(8)
F(8)	10 669(15)	4 679(6)	6 716(14)
N(01)	5 623(13)	7 690(8)	2 852(14)
C(01)	6 540(15)	7 477(8)	3 562(13)
C(02)	7 690(15)	7 191(9)	4 348(15)

* Invariant parameter.

excess HBF_4 . The solvent was then removed and the residue extracted into MeCN which was concentrated and cooled to give $[\text{Mo}(\eta^5\text{-C}_5\text{H}_5)_2(\text{MeCN})(\text{NH}=\text{CHMe})][\text{BF}_4]_2$ (2) as deep red plates which darken above 150 °C. Yield: ca. 95% (0.48 g). I.r.: 2 320m and 1 655m cm^{-1} . N.m.r.: ^1H , δ 2.15 [d of d,

CH_3CHNH , $^3\text{J}(\text{CH}_3\text{-CH})$ 5.08, $^4\text{J}(\text{CH}_3\text{-NH})$ 1.61], 2.35 (s, CH_3CN), 5.86 (s, C_5H_5), 7.80 [d of quartets, MeCHNH , $^3\text{J}(\text{CH-CH}_3)$ 5.08, $^3\text{J}(\text{CH-NH})$ 20.9], 9.19 [br d, MeCHNH , $^3\text{J}(\text{NH-CH})$ 20.9]; $^{13}\text{C}\{-^1\text{H}\}$, δ 6.58 (CH_3CHNH), 27.0 (CH_3CN), 102.7 (C_5H_5), 103.3 (MeCHNH), 193.0 (MeCN).

2. *Bis*(η^5 -cyclopentadienyl)*bis*(trimethylphosphine)molybdenum(IV) Tetrafluoroborate (3).—To the above cyclopentadienyl compound [(2)] (0.25 g, 0.65 mmol) was added PMe_3 (0.2 cm^3 , 2 mmol) at 0 °C, whereupon the colour changed from red to yellow as the solid dissolved. After removal of excess PMe_3 the residue was extracted into MeCN, which was concentrated and cooled to give yellow prisms. Yield: essentially quantitative. N.m.r.: ^1H , δ 1.60 [d, PMe_3 , $^2\text{J}(\text{P-H})$ 6.6] and 5.48 [t, C_5H_5 , $^3\text{J}(\text{P-H})$ 2]; $^{31}\text{P}\{-^1\text{H}\}$, δ 10.38 (s, PMe_3).

3. *Interaction of* $\text{Mo}(\text{CO})_3(\text{MeCN})_3$ *with Tetrafluoroboric Acid.*—(a). To $\text{Mo}(\text{CO})_3(\text{MeCN})_3$ ¹² (1.0 g, 3.2 mmol) in MeCN (50 cm^3) was added $\text{HBF}_4 \cdot \text{Et}_2\text{O}$ (2 cm^3 , 50% solution) dropwise over ca. 5 min under an argon atmosphere. Gas evolution occurred and the initial orange solution was stirred for 20 h, becoming greenish in colour; the solvent was removed and the residue extracted into MeCN (20 cm^3). The filtered solution was concentrated and cooled at -20 °C for ca. 12 h to give orange crystals of $[\text{Mo}(\text{CO})_2(\text{MeCN})_3(\eta^3\text{-CH}_2\text{CHNH}_2)]\text{-BF}_4$ (4) which were collected and dried. Yield 0.61 g, 46%. When the reaction is carried out under dihydrogen the yield of complex (4) is 1.01 g, 76%. I.r.: 2 315m, 2 287m, 1 942s, and 1 860s cm^{-1} . ^1H N.m.r. (CD_3CN): δ 1.47 (d, CH_2 , J 9.84), 1.93 (s, MeCN), 3.56 (d, NH_2 , J 6.58), and 4.02 (overlapping t of t, CH, J 9.84, 6.58).

(b). After removal of the aza-allyl, further concentration and cooling of the solution leads to dark green needles of $[\text{Mo}_2(\mu\text{-O})(\text{MeCN})_{10}][\text{BF}_4]_4$ (5) in ca. 25% yield. However, the following procedure is recommended.

To $\text{Mo}(\text{CO})_3(\text{MeCN})_3$ (1.35 g, 4.45 mmol) in MeCN (50 cm^3) was added $\text{HBF}_4 \cdot \text{OEt}_2$ (2.8 cm^3 , 50% solution) dropwise and the orange solution stirred under air for 2 h during which time the solution became dark green. Reduction to ca. 15 cm^3 followed by addition of Et_2O (49 cm^3) gave a green precipitate which was collected, washed with Et_2O ($3 \times 10 \text{ cm}^3$), and dried in vacuum. Recrystallisation from MeCN gave dark green needles. Yield: 1.89 g, 88%. I.r.: 2 305vw, 2 185m, and 2 150s cm^{-1} (MeCN). Raman spectrum in MeCN: $\nu(\text{Mo-O-Mo})$ 341.0 cm^{-1} (green line 514.5 nm). ^1H N.m.r. (CD_3CN): δ 1.9 (br). Conductivity: $\Lambda_{\text{M}}(\text{MeCN}) = 552 \text{ ohm}^{-1} \text{ cm}^2 \text{ mol}^{-1}$.

X-Ray Crystallography.—Crystals of all four compounds were sealed under argon in thin-walled glass capillaries. Compounds (3) and (5) were solvated by one and two molecules of MeCN, respectively. Following preliminary photography, orientation matrices, cell dimensions, and intensity data were obtained using a CAD4 diffractometer, operating in the ω - 2θ scan mode with graphite monochromatised Mo-K_α radiation ($\lambda = 0.710 69 \text{ \AA}$) as previously described.¹³ The structures were

solved *via* the heavy-atom method and refined using full-matrix least squares. For all compounds, the BF_4 groups showed high thermal motion, but for compound (2) it proved impossible reliably to identify BF_4 tetrahedra. Accordingly, the fluorine content was modelled by inserting partial atoms at all sites showing significant electron density on a difference map phased without fluorine contribution, with occupancy factors proportional to the electron density indicated, but with an overall sum equal to four fluorines per boron.

Crystal data and details of the analysis and refinement are given in Table 6. Final fractional atomic co-ordinates are given in Tables 7–10. Additional material available from the Cambridge Crystallographic Data Centre comprises H-atom co-ordinates, thermal parameters, and remaining bond lengths and angles.

Acknowledgements

We thank the S.E.R.C. for a studentship (to B. S. M.) and provision of X-ray facilities and British Petroleum for assistance with research expenses. We thank Mr. W. Ali for assistance with Raman spectra.

References

- 1 T. C. Wright, G. Wilkinson, M. Motevalli, and M. B. Hursthouse, *J. Chem. Soc., Dalton Trans.*, 1986, 2017; see also, P. A. Chetcuti, C. B. Knobler, and M. F. Hawthorne, *Organometallics*, 1988, 7, 650.
- 2 A. R. Barron, J. E. Salt, G. Wilkinson, M. Motevalli, and M. B. Hursthouse, *J. Chem. Soc., Dalton Trans.*, 1987, 2947 and refs. therein.
- 3 J. L. Thomas, *J. Am. Chem. Soc.*, 1975, 97, 5943.
- 4 S. M. B. Costa, A. R. Dias, and F. J. S. Pina, *J. Organomet. Chem.*, 1979, 175, 193.
- 5 T. Aviles, M. L. H. Green, A. R. Dias, and C. Romero, *J. Chem. Soc., Dalton Trans.*, 1979, 1367.
- 6 M. Green, R. J. Mercer, C. E. Morton, and A. G. Orpen, *Angew. Chem., Int. Ed. Engl.*, 1985, 24, 422.
- 7 F. A. Cotton and G. Wilkinson, 'Advanced Inorganic Chemistry,' 5th edn., John Wiley and Sons, New York, 1985, pp. 1197, 1217.
- 8 E. I. Stiefel, C. D. Garner, G. Pimblett, A. G. Sykes, R. L. Richards, and G. J. Leigh, 'Comprehensive Coordination Chemistry,' eds. G. Wilkinson, R. D. Gillard, and E. W. Abel, Pergamon Press, Oxford, 1987, vol. 3.
- 9 J. A. Bloomhead, M. Sterns, and C. G. Young, *J. Chem. Soc., Chem. Commun.*, 1981, 1262.
- 10 See ref. 7, p. 466.
- 11 J. R. Campbell and R. J. H. Clarke, *Mol. Phys.*, 1978, 36, 1133.
- 12 D. P. Tate, W. R. Knipple, and J. M. Augl, *Inorg. Chem.*, 1962, 1, 433.
- 13 R. A. Jones, M. B. Hursthouse, K. M. A. Malik, and G. Wilkinson, *J. Am. Chem. Soc.*, 1979, 101, 4128.

Received 15th July 1987; Paper 7/1267